International Journal of Informatics and Computation (IJICOM)
Vol. 8, No. 1, 2026
ISSN: 2685-8711, E-ISSN: 2714-5263 DOI: 10.35842/ijicom

Automatic Tuberculosis Classification in Sputum using YOLOv12 and IUATLD

Nia Saurina[1], Lestari Retnawati[2], Firman hadi Sukma Pratama[3], Teguh Pribadi Ikhsan[4]

Abstract
Tuberculosis remains a major global health challenge, particularly in resource-limited regions where rapid and accurate diagnosis is still difficult to achieve. This paper proposes an automated deep-learning framework for the detection, quantification, and classification of Acid-Fast Bacilli (AFB) in sputum smear images to address the limitations of conventional manual microscopy, which is labor intensive, time-consuming, and prone to inter-observer variability. Our proposed method utilizes the YOLOv12 object detection architecture to identify tuberculosis bacilli from Ziehl–Neelsen-stained sputum images. We use a carefully annotated dataset prepared by expert microbiologists based on the International Union Against Tuberculosis and Lung Disease (IUATLD) grading standard. The experimental results show that the proposed model achieves strong detection performance with a mean Average Precision (mAP) of 84.7%, precision of 74.18%, recall of 73.90%, and F1-score of 74.04%. Furthermore, this paper maps the detected bacilli counts into standardized IUATLD diagnostic categories, including Scanty, 1+, 2+, and 3+, to ensure compatibility with routine clinical reporting procedures. The obtained results demonstrate that our proposed system can provide accurate, consistent, and efficient tuberculosis screening support. This study confirms that integrating YOLOv12 with IUATLD grading can produce a scalable and reliable automated diagnostic framework for improving TB microscopy analysis in high-burden laboratory environments.

Keywords:
Mycobacterium Tuberculosis, YOLOv12, IUATLD, Classification

1. Introduction

Tuberculosis (TB) remains one of the most serious infectious diseases worldwide and continues to create major public health challenges, especially in developing countries. The disease spreads through airborne transmission and often requires rapid diagnosis to prevent further infection and reduce mortality rates. Conventional TB diagnosis commonly relies on sputum smear microscopy, chest X-ray examination, and molecular testing. However, manual microscopic examination requires experienced laboratory personnel and often produces inconsistent results due to human subjectivity and fatigue. Several studies also report that delayed diagnosis contributes to treatment failure and increases the transmission rate within communities. These conditions encourage researchers to develop automated and intelligent diagnostic systems that can support medical personnel in identifying TB cases more efficiently and accurately [1], [2], [5], [31].

Sputum smear microscopy using Ziehl–Neelsen staining remains one of the most widely used laboratory techniques for pulmonary tuberculosis detection because of its low

Corresponding Author: Nia Saurina(niasaurina@gmail.com)
1 Nia Saurina, Universitas Wijaya Kusuma Surabaya, niasaurina@gmail.com
2 Lestari Retnawati, Universitas Wijaya Kusuma Surabaya, Lestari.047@gmail.com
3. Firman Hadi Sukma Pratama, Universitas Wijaya Kusuma Surabaya, firmanpratama@uwks.ac.id
4 Teguh Pribadi Ikhsan, Universitas Wijaya Kusuma Surabaya, teguh@uwks.ac.id

operational cost and accessibility in many healthcare facilities. Despite its practicality, this method still depends heavily on manual observation under a microscope, which often leads to variability in interpretation between examiners. Researchers identify several challenges in sputum analysis, including overlapping bacilli structures, inconsistent staining quality, and variations in illumination conditions during image acquisition. In addition, laboratory workloads frequently reduce examination consistency and increase the possibility of diagnostic errors. Recent studies on digitized sputum smear datasets demonstrate the importance of developing automated image-based classification systems that can improve reproducibility and accelerate microscopic examination processes. [3], [13], [14], [31]

Artificial intelligence and deep learning technologies increasingly support medical image analysis because they can automatically learn complex visual patterns from large datasets. Many healthcare applications utilize deep learning approaches to improve disease diagnosis, lesion segmentation, and abnormality detection in medical images. Previous studies successfully apply deep learning to lung cancer detection, diabetic ulcer analysis, tumor classification, and pulmonary disease diagnosis with promising accuracy levels. These approaches demonstrate that neural networks can extract discriminative visual features that are difficult to identify manually. However, the performance of deep learning systems strongly depends on dataset quality, model architecture, and computational optimization strategies. Therefore, researchers continue exploring more robust object detection architectures to achieve better performance in medical imaging tasks. [16], [17], [18], [32]

Object detection models based on the YOLO (You Only Look Once) architecture gain significant attention because they provide high detection speed and competitive accuracy in real-time applications. YOLO-based systems perform object localization and classification simultaneously in a single-stage detection framework, making them highly efficient for medical and industrial image analysis. Previous studies apply YOLO architectures for pneumonia detection, retinal pathology analysis, underwater object detection, drone recognition, and lung nodule localization. Researchers also report that newer YOLO variants improve feature extraction capability, computational efficiency, and small-object detection performance through attention mechanisms and lightweight optimization strategies. These advancements indicate that YOLO-based models have strong potential for automated TB bacilli detection in microscopic sputum images. [11], [12], [19], [23], [24], [27], [28], [34], [35]

Several studies specifically investigate the application of YOLO architectures in tuberculosis detection using chest X-ray images. Researchers demonstrate that YOLO-based systems can effectively identify TB-related abnormalities and support computer-aided diagnosis in pulmonary imaging. Other studies also highlight the capability of artificial intelligence-based computer-aided detection systems to improve TB screening performance in community healthcare programs. However, most existing works focus on radiographic imaging rather than direct sputum smear analysis. Chest X-ray analysis often requires expensive imaging equipment and may not provide direct visualization of Mycobacterium tuberculosis bacteria. Consequently, automated sputum image classification remains an important research area, particularly for healthcare facilities with limited radiological resources. [9], [15], [30], [32], [36], [37]

The International Union Against Tuberculosis and Lung Disease (IUATLD) grading system plays a crucial role in standardizing sputum smear examination results. This grading system categorizes TB infection severity based on the number of acid-fast bacilli identified during microscopic observation. The IUATLD standard helps healthcare professionals maintain diagnostic consistency and supports treatment monitoring processes. However, manual implementation of IUATLD grading still depends on visual counting performed by laboratory experts, which introduces potential inconsistencies and time inefficiencies. Recent digitized sputum smear studies emphasize the importance of

integrating automated image analysis with IUATLD classification standards to produce objective and reproducible diagnostic outcomes. Therefore, combining deep learning object detection with IUATLD grading becomes a promising approach for automated TB classification systems. [13], [14], [31]

Recent advancements in object detection architectures encourage researchers to explore more adaptive and accurate YOLO variants for healthcare applications. Improved versions of YOLO introduce lightweight backbone networks, hybrid attention modules, deformable kernels, and optimized feature fusion mechanisms to enhance detection capability under complex image conditions. Studies show that these architectural improvements increase detection precision for small objects and noisy environments while maintaining computational efficiency. Since TB bacilli in sputum images often appear as very small objects with varying orientations and staining intensities, robust detection models become essential for achieving reliable classification performance. These developments motivate the use of newer YOLO architectures such as YOLOv12 for microscopic TB image analysis. [22], [23], [24], [25], [26], [34], [35]

Based on these challenges and technological developments, this study focuses on developing an automatic tuberculosis classification system in sputum images using the YOLOv12 architecture integrated with the IUATLD grading standard. This study aims to improve the efficiency, consistency, and accuracy of TB detection by automatically identifying bacilli patterns from microscopic sputum smear images. We utilize deep learning-based object detection to support laboratory examination processes and reduce dependency on manual interpretation. The proposed approach is expected to provide faster diagnostic assistance for healthcare workers while supporting standardized TB classification procedures in clinical environments. Furthermore, this study contributes to the growing application of artificial intelligence in medical image analysis, particularly in automated infectious disease detection systems. [14], [15], [23], [30], [36].

2. Related Works

Previous studies investigated the implementation of artificial intelligence for tuberculosis diagnosis using predictive and machine learning approaches. Osamor and Okezie developed an ensemble-based predictive system for tuberculosis diagnosis and reported that weighted voting algorithms improved classification reliability and diagnostic consistency. Their work demonstrated that machine learning models could support healthcare decision-making processes effectively. However, the study focused primarily on structured clinical data rather than medical image analysis. The proposed approach also did not address microscopic sputum examination, which remains one of the most widely used TB diagnostic methods in many healthcare facilities. [8]

Several researchers explored computer vision techniques for pulmonary disease detection using chest radiography images. Mustafa and Nsour applied computer vision methods for abnormality detection in chest X-rays and showed that automated image analysis improved diagnostic support performance. Rahamathulla et al. further implemented YOLOv8 for tuberculosis identification from chest images and obtained promising detection accuracy with efficient processing time. Similarly, Bista et al. utilized YOLOv7 for chest X-ray tuberculosis detection and demonstrated that real-time object detection architectures effectively identified pulmonary abnormalities. Although these studies produced strong classification performance, they relied heavily on radiographic imaging and did not focus on direct bacilli detection from sputum smear microscopy. [9], [15], [30]

Research on sputum smear image analysis became increasingly important because sputum microscopy directly visualizes Mycobacterium tuberculosis bacteria. Martín-Higuera et al. analyzed sputum bacillary burden using Xpert MTB/RIF Ultra and confirmed the importance of bacilli quantification for pulmonary tuberculosis assessment. Aulia et al.

later introduced a digitized microscopic sputum smear dataset based on IUATLD grades and developed a classification framework for Ziehl–Neelsen stained sputum images. Their study provided an important contribution to automated sputum analysis because it standardized microscopic image classification according to IUATLD grading criteria. However, the study mainly emphasized dataset development and conventional classification analysis rather than advanced real-time object detection models. [13], [14]

Researchers also examined the effectiveness of YOLO architectures in different object detection domains. Alkentar et al. compared YOLO, SSD, and Faster R-CNN for drone detection and found that YOLO achieved superior detection speed while maintaining competitive accuracy. Lavanya and Pande improved real-time object detection performance using optimized YOLO frameworks and showed that single-stage detectors efficiently handled dynamic object recognition tasks. These findings highlighted the advantage of YOLO models in balancing computational efficiency and detection precision. Nevertheless, these studies focused on general object detection scenarios and did not evaluate microscopic medical images containing small and overlapping biological objects. [11], [19]

Several studies improved YOLO architectures through lightweight optimization and attention-based enhancement techniques. Jooshin et al. proposed Inception-YOLO and improved YOLOv5 performance by integrating modified inception and CSP modules. Fang and Yang developed a lightweight YOLOv8 architecture for wheat head detection and achieved higher efficiency while reducing computational complexity. Gao et al. also introduced GCP-YOLOv7 for underwater target detection and improved small-object recognition capability through feature optimization. These studies demonstrated that architectural modifications significantly improved object detection robustness under complex visual conditions. However, their implementations targeted agricultural and underwater datasets rather than microscopic medical imaging applications. [23], [24], [25]

Deep learning methods also showed promising results in broader medical image analysis applications. Huang et al. implemented deep learning object detection for early lung cancer detection and achieved effective lesion localization in medical imaging datasets. Hussain et al. reviewed multimodality tumor detection systems and concluded that deep learning models substantially improved classification performance in diagnostic imaging tasks. Fati et al. further combined deep and hybrid learning techniques for tuberculosis detection using chest X-ray images and demonstrated that feature fusion improved diagnostic accuracy [16], [18], [32].

Researchers also investigated the role of artificial intelligence in automated healthcare screening systems. Okada et al. evaluated artificial intelligence-based computer-aided detection systems for pulmonary tuberculosis screening and found that AI-assisted approaches improved community-based active case finding performance. Manoli et al. reviewed advancements in deep learning for tuberculosis detection and highlighted the effectiveness of modified CNN architectures and transfer learning techniques in pulmonary disease diagnosis. However, they identified several limitations, including insufficient evaluation on microscopic sputum datasets and limited exploration of real-time object detection architectures for bacilli identification. [36], [37]

Based on previous studies, most tuberculosis detection research focused on chest radiography analysis, while fewer studies explored automatic sputum smear classification integrated with standardized IUATLD grading. Existing works also rarely investigated the implementation of newer YOLO architectures for microscopic bacilli detection. Therefore, this study addressed these gaps by utilizing YOLOv12 for automatic tuberculosis classification in sputum smear images based on IUATLD standards. This study combined real-time object detection capability with microscopic image analysis to improve diagnostic consistency, accelerate examination processes, and support laboratory-based tuberculosis screening systems. [14], [15], [23], [30].

3. Proposed Method

This research developed an automated diagnostic system to detect, classify, and quantify Mycobacterium tuberculosis bacilli in digitized sputum smear images. The pipeline integrates a state-of-the-art deep learning object detector with a rule-based module that translates quantitative outputs into the standardized International Union Against Tuberculosis and Lung Disease (IUATLD) grading scale. The methodology comprises five sequential stages: (1) dataset acquisition and description, (2) expert annotation and preprocessing, (3) model architecture and training protocol, (4) post-processing for IUATLD grade assignment, and (5) comprehensive performance evaluation, as seen in Fig. 1.

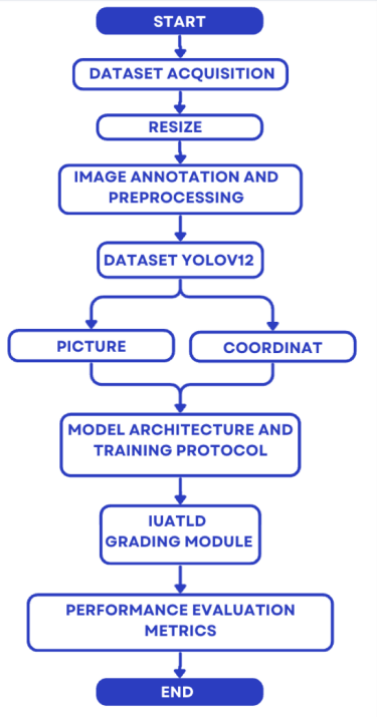

Fig. 1. Research Method

The model was developed and validated using a curated dataset of Ziehl–Neelsen (ZN)-stained sputum smear microscopy images. All samples were obtained from the Clinical Pathology Department of Dr. Soetomo Hospital, Universitas Airlangga, Indonesia. The dataset comprised 1,265 high-resolution digital images captured under 1000x oil-immersion microscopy, reflecting real-world variability in smear thickness, staining intensity, and bacilli density. This diversity is crucial for training a robust model capable of generalizing across different laboratory conditions. The use of retrospective, anonymized samples was approved by the relevant institutional ethics committee.

A critical prerequisite for supervised deep learning is high-quality labeled data. Each M. tuberculosis bacillus in every image was manually annotated by certified microbiologists using rectangular bounding boxes. This expert-led process ensured clinical validity and adherence to morphological criteria for identifying acid-fast bacilli (AFB). The annotations were performed using Bounding Box, and the coordinates for each bounding box were saved in the YOLO format [28-30]. This format consists of the object class ID followed by the normalized center-x, center-y, width, and height values relative to the image dimensions. This research had four scenario to all images and their corresponding annotations were subsequently partitioned into training, validation, and test sets using a

structured split (1) 60:20:20, (2) 70:15:15, (3) 80:10:10, (4) 90:5:5. Standard preprocessing steps were applied uniformly, including image resizing to the model's native input dimensions in 640x480 pixels and normalization of pixel intensity values to a "0" to "1" range to stabilize and accelerate the training process.

In this study, we utilize the YOLOv12 architecture as the core object detection model to automatically identify tuberculosis bacilli in sputum smear images. This approach applies a convolutional neural network backbone to extract hierarchical image features, followed by a neck module for multi-scale feature fusion and a detection head that simultaneously performs object classification and bounding box regression. The model produces the number of detected bacilli within each microscopic field, and the detection results are further processed through a deterministic post-processing stage to generate clinically interpretable outputs based on IUATLD grading standards. To evaluate system performance, this study applies a two-level evaluation framework consisting of technical and clinical assessment metrics. The technical evaluation uses Precision, Recall, F1-score, and mean Average Precision (mAP) to measure the model's capability in localizing and detecting bacilli accurately. Furthermore, this approach evaluates diagnostic performance by comparing the predicted bacilli counts and IUATLD classification results with expert-annotated ground truth data to ensure the reliability and clinical relevance of the proposed automated TB detection system.

The proposed YOLOv12-based tuberculosis detection system can be mathematically formulated as follows:

The input sputum image is represented as:

$$X \in R^{H \times W \times C}$$

where X denotes the microscopic sputum image with height H, width W, and color channels C.

The YOLOv12 model extracts image features and performs object detection using:

$$\hat{Y} = f(X; \theta)$$

where $f(.)$ represents the YOLOv12 detection model and θ denotes the trainable network parameters. The output $\hat{Y}$ contains predicted bounding boxes, confidence scores, and bacilli class labels.

The bounding box prediction is defined as:

$$B_i = (x_i, y_i, w_i, h_i, c_i)$$

where (x_i, y_i) represent the center coordinates, w_i and h_i denote the width and height of the detected bacillus region, and c_i indicates the confidence score.

The total detected bacilli count is calculated as:

$$N = \sum_{i=1}^{n} B_i \quad (1)$$

where N represents the total number of detected tuberculosis bacilli within the microscopic field.

The IUATLD classification is then determined using:

$$G = g(N)$$

where G denotes the final IUATLD grade generated from the bacilli count N.

To evaluate model performance, Precision and Recall are computed as:

$$Precision = \frac{TP}{TP + FP} \quad (2)$$

$$Recall = \frac{TP}{TP + FN} \tag{3}$$

where TP is true positive detection, FP is false positive detection, and FN is false negative detection.
The F1-score is calculated using:

$$F1 = 2 \times \frac{Precision \times Recall}{Precision + Recall} \tag{4}$$

This formulation allows the proposed system to automatically detect bacilli, estimate infection severity based on IUATLD standards, and quantitatively evaluate the detection performance of the YOLOv12 model.

4. Result and Analysis

This section presents the quantitative results obtained from the proposed automated tuberculosis detection and IUATLD grading system. This study can produce automatic identification and classification of *Mycobacterium tuberculosis* bacilli using the YOLOv12 object detection model integrated with IUATLD-based diagnostic grading. The system performance is evaluated through object detection capability and clinical grading accuracy. In this study, the model is trained and validated using 1,265 Ziehl–Neelsen-stained sputum smear images. The training process utilizes an input image resolution of 640 × 640 pixels with a batch size of 16 and continues iteratively until the validation loss reaches convergence, ensuring stable and optimal detection performance.

Fig. 2 presents the detection results generated by the proposed YOLOv12-based artificial intelligence model on digital sputum microscopy images. In this study, we obtain multiple detected objects classified as *Mycobacterium tuberculosis* bacilli, where each detected region is labeled as “TBbacillus” along with a confidence score ranging from 0 to 1. Our proposed system produces varying confidence values between approximately 0.41 and 0.75, indicating different levels of detection certainty based on bacilli morphology, staining quality, and image complexity. Higher confidence scores represent clearer and more reliable bacilli detection, while lower scores indicate uncertain detections caused by overlapping objects, weak staining, or irregular bacilli shapes. To improve detection reliability and reduce false positive predictions, this approach applies a confidence threshold mechanism in which only detections above the predefined threshold are accepted for the final bacilli counting and IUATLD classification process.

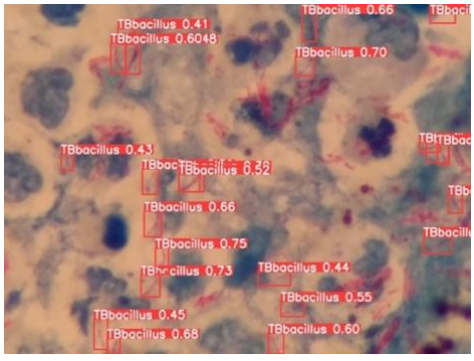

Fig 2. Result of training the Image of Mycobacterium Tuberculosis with YOLOv12

Table 3 presents an analysis of 13 patients, detailing the number of tuberculosis (TB) bacteria observed across 100 microscopic fields. For each patient, the table specifies the total TB count, the number of fields showing a 2+ density, and the number of fields showing a 3+ density. Based on these values, an IUATLD (International Union Against Tuberculosis and Lung Disease) score is assigned. The majority of patients (1 through 12) exhibit high total bacterial loads, ranging from 95 to 99 per 100 fields. Consequently, most of these patients received a score of 3+, although patients 2, 4, and 9 received a score of 2+. Patient 13 stands out as a clear exception, with a significantly lower total count of 36, resulting in a 1+ score. This single outlier contrasts sharply with the consistently high counts and scores of the other twelve subjects. This IUATLD result are given in second scenario which is 70:15:15.

Table 3. IUATLD's Result in Second Scenario

Patient	10-99 BTA in 100 fields of view	1-10 BTA in 100 field of view	More Than 10 BTA in 1 field of view	Skor IUATLD
1	99	74	25	3+
2	97	81	16	2+
3	99	77	22	3+
4	98	80	18	2+
5	97	76	21	3+
6	95	72	23	3+
7	99	73	26	3+
8	98	71	27	3+
9	97	78	19	2+
10	99	78	21	3+
11	96	75	21	3+
12	99	78	21	3+
13	36	27	9	1+

Fig 3 shows the Tuberculosis Classification Training Results using the YOLOv12 method on 70:15:15 partitioned data, with a Precision value reaching 74.18% indicated by the blue graph, Recall reaching 73.90% indicated by the green graph, F1-Score reaching 74.04% indicated by the red graph, Accuracy reaching 69.26% indicated by the purple graph, and mAP50 of 84.7% indicated by the orange graph.

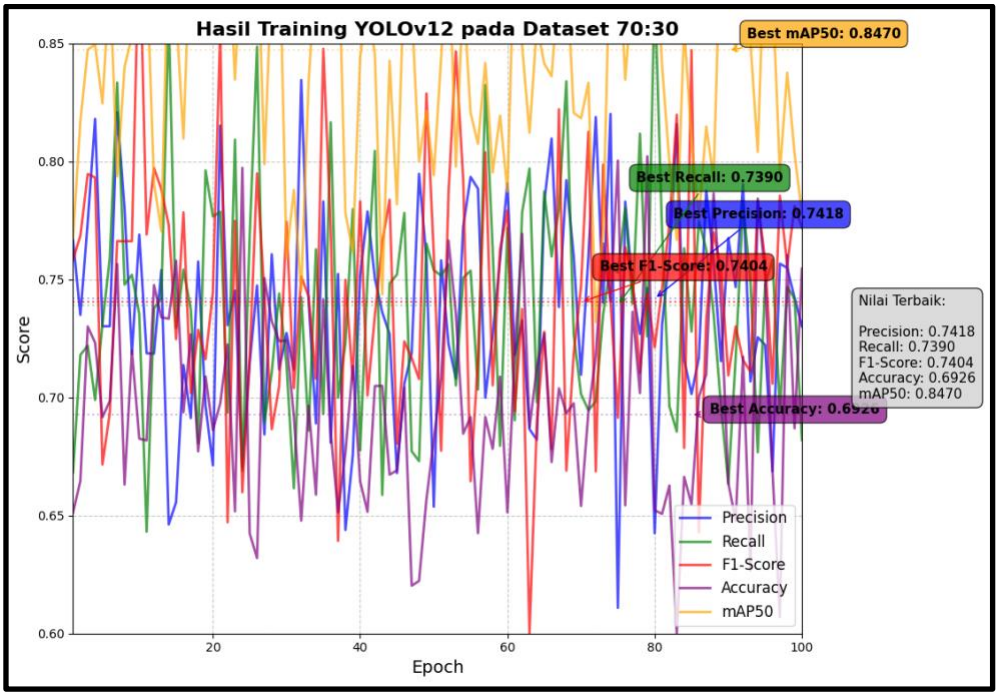

Fig 3. Tuberculosis Classification Training Results using the YOLOv12 method on 70:15:15 partitioned data

The results demonstrate that this research successfully develops a fully automated pipeline capable of detecting, quantifying, and classifying *Mycobacterium tuberculosis* bacilli in sputum smear images using the YOLOv12 architecture integrated with the IUATLD grading standard. The proposed system shows that combining deep learning object detection with standardized clinical grading is technically feasible and clinically meaningful. The experimental results indicate that the model achieves strong detection capability with high precision, recall, and mAP performance, confirming its ability to identify bacilli accurately while minimizing false detections. Furthermore, the consistent performance across validation datasets demonstrates that the model maintains robustness against variations in staining quality, smear density, and image acquisition conditions.

This study also highlights the clinical relevance of transforming object detection outputs into standardized diagnostic information. The proposed approach automatically converts detected bacilli counts into IUATLD grading categories such as Scanty, 1+, 2+, and 3+, allowing the system to generate clinically interpretable results that align with laboratory diagnostic procedures. The high agreement between automated predictions and expert annotations indicates that the system can replicate manual microscopic assessment with consistent performance. This capability provides significant advantages over traditional manual microscopy because the proposed system offers faster analysis, objective interpretation, and reduced diagnostic variability. In addition, the automated framework supports laboratory efficiency by reducing technician workload and enabling more standardized tuberculosis screening processes, particularly in high-burden and resource-limited healthcare environments.

Although the proposed system demonstrates promising performance, several limitations remain important for future improvement. The detection accuracy strongly depends on the diversity and quality of the training dataset, including staining consistency, bacilli visibility, and image clarity. Difficult cases such as overlapping bacilli structures, excessive debris, and poor smear preparation still affect the reliability of object localization and counting accuracy. Furthermore, this study validates the model using a dataset of

1,265 sputum smear images, but additional evaluation using external datasets from different laboratories and geographic regions is necessary to ensure broader generalization capability. Future work may focus on improving lightweight model optimization, enhancing small-object detection performance, and integrating the proposed system into a user-friendly clinical software platform to support routine laboratory implementation and real-time tuberculosis diagnosis.

5. Conclusion

This study develops and validates an automated deep-learning system for detecting, quantifying, and grading *Mycobacterium tuberculosis* in Ziehl–Neelsen-stained sputum smear images. Our proposed method utilizes the YOLOv12 object detection model integrated with the IUATLD grading standard to produce clinically interpretable diagnostic results. The system successfully addresses the limitations of conventional manual microscopy, which often requires extensive time, expert interpretation, and repetitive laboratory procedures. Based on the experimental evaluation, the proposed model achieves strong detection performance with a mean Average Precision (mAP) of 84.7%, precision of 74.18%, recall of 73.90%, and F1-score of 74.04%. These findings indicate that the proposed framework can reliably identify tuberculosis bacilli under varying smear conditions and image characteristics.

This paper further demonstrates that integrating deep learning detection outputs with the IUATLD grading protocol can effectively transform raw bacilli counts into standardized clinical categories, including Scanty, 1+, 2+, and 3+. The proposed approach provides a direct bridge between artificial intelligence analysis and routine laboratory workflows, allowing the system to generate objective and consistent diagnostic interpretations. In addition, this study confirms that the automated grading mechanism can support laboratory personnel in reducing diagnostic variability while improving efficiency and throughput in tuberculosis screening activities. The obtained results highlight the potential of artificial intelligence to support faster and more scalable tuberculosis diagnosis, particularly in high-burden healthcare environments.

Although the proposed system achieves promising results, this study recognizes several limitations related to dataset diversity, staining variability, and challenging microscopic conditions such as overlapping bacilli and image artifacts. Our proposed method still depends on the quality and representativeness of the training dataset, which may influence generalization across different laboratory settings. Therefore, future work should expand the dataset using multi-center clinical samples and investigate more adaptive detection architectures to further improve robustness and grading consistency. Overall, this paper demonstrates that combining YOLO-based object detection with standardized IUATLD classification can produce an effective and clinically relevant automated tuberculosis diagnostic framework for digital microscopy applications.

References

[1] Salifu, R. S. and Hlongwana, K. "Frontline healthcare workers' experiences in implementing the tb-dm collaborative framework in northern ghana". BMC Health Services Research, Vol. 21, No. 1. 2021. https://doi.org/10.1186/s12913-021-06883-6

[2] Gezahegn, H., Ibrahim, M. A., & Mulat, E. "Diabetes Mellitus and Tuberculosis Comorbidity and Associated Factors Among Bale Zone Health Institutions, Southeast Ethiopia". Diabetes, Metabolic Syndrome and Obesity: Targets and Therapy, Volume 13. 2020. https://doi.org/10.2147/dmso.s248054

[3] Prayuni, K., Razari, I., Nihayah, S., & Yuliwulandari, R. "The use of high resolution melting (HRM) method to detect rs1800629 of tumor necrosis factor-alpha (tnf-alpha) gene among

tuberculosis patients". Medical Laboratory Technology Journal, Vol. 7, No. 1. 2021. https://doi.org/10.31964/mltj.v7i1.362
[4] Melinda, M., Olivianto, E., & Kusuma, H. C. "Correlation of regulatory t cells percentage and lung tuberculosis in children". Pediatrics Sciences Journal, Vol 2, No. 1. 2022. https://doi.org/10.51559/pedscij.v2i1.21
[5] Diniawati, E. and Wibowo, A. "The economic burden and non-adherence tuberculosis treatment in indonesia: systematic review". KnE Life Sciences, Vol 4, No. 10. 2019. https://doi.org/10.18502/kls.v4i10.3703
[6] Penjor, D. and Pradhan, B. "Diagnostic dilemma in a patient with nasopharyngeal tuberculosis: a case report and literature review". SAGE Open Medical Case Reports, 2022. https://doi.org/10.1177/2050313x221131389
[7] Kim, Y., Lee, D., Hwang, H., & Kim, M. "En plaque tuberculoma: a case report. Investigative Magnetic Resonance Imaging", Vol 20, No. 3. 2016. https://doi.org/10.13104/imri.2016.20.3.200
[8] Osamor, V. C. and Okezie, A. F. "Enhancing the weighted voting ensemble algorithm for tuberculosis predictive diagnosis". Scientific Reports, Vol. 11, No. 1. 2021. https://doi.org/10.1038/s41598-021-94347-6
[9] Mustafa, Z. and Nsour, H. (2023). Using computer vision techniques to automatically detect abnormalities in chest x-rays. Diagnostics, 13(18), 2979. https://doi.org/10.3390/diagnostics13182979
[10] Azizah, N., Sahria, Y., Sahwari, S., & Iskandar, M. (2023). Car vehicle image object detection using you only live once (yolo). Anterior Jurnal, 22(3), 211-216. https://doi.org/10.33084/anterior.v22i3.5577
[11] Lavanya, G. and Pande, S. D. (2023). Enhancing real-time object detection with yolo algorithm. EAI Endorsed Transactions on Internet of Things, 10. https://doi.org/10.4108/eetiot.4541
[12] Munna, M. S., -, R. C., & Siddiqee, A. M. (2024). A comparative study of yolo models for pneumonia detection. International Journal for Multidisciplinary Research, 6(3). https://doi.org/10.36948/ijfmr.2024.v06i03.22770
[13] Martín-Higuera, M. C., Rivas, G. A., Rolo, M., Muñoz-Gallego, I., & López-Roa, P. (2023). Xpert MTB/RIF Ultra CT value provides a rapid measure of sputum bacillary burden and predicts smear status in patients with pulmonary tuberculosis. Scientific Reports, 13(1). https://doi.org/10.1038/s41598-023-28869-6
[14] Aulia, S., Suksmono, A. B., Mengko, T. R., & Alisjahbana, B. (2024). A Novel Digitized Microscopic Images of ZN-Stained Sputum Smear and Its Classification Based on IUATLD Grades. IEEE Access, 12, 51364-51380. https://doi.org/10.1109/access.2024.3386208
[15] Rahamathulla, M. P., Emmanuel, W. R. S., Bindhu, A., & Ahmed, M. M. (2024). YOLOv8's advancements in tuberculosis identification from chest images. Frontiers in Big Data, 7. https://doi.org/10.3389/fdata.2024.1401981
[16] Huang, K., Chung, C., & Xu, J. (2025). Deep learning object detection-based early detection of lung cancer. Frontiers in Medicine, 12. https://doi.org/10.3389/fmed.2025.1567119
[17] Zhang, J., Qiu, Y., Peng, L., Zhou, Q., Wang, Z., & Qi, M. (2022). A comprehensive review of methods based on deep learning for diabetes-related foot ulcers. Frontiers in Endocrinology, 13. https://doi.org/10.3389/fendo.2022.945020
[18] Hussain, D., et, al. (2024). Revolutionizing tumor detection and classification in multimodality imaging based on deep learning approaches: Methods, applications and limitations. Journal of X-Ray Science and Technology Clinical Applications of Diagnosis and Therapeutics, 32(4), 857-911. https://doi.org/10.3233/xst-230429
[19] Alkentar, S., Alsahwa, B., Assalem, A., & Karakolla, D. (2021). Practical comparation of the accuracy and speed of YOLO, SSD and Faster RCNN for drone detection. Journal of Engineering, 27(8), 19-31. https://doi.org/10.31026/j.eng.2021.08.02
[20] Tiwari, S. (2025). Advanced Two Stage AI Technique for Object Detection. International Journal of Scientific Research in Engineering and Management, 09(05), 1-9. https://doi.org/10.55041/ijsrem47821
[21] Zhang, J., Qiu, Y., Peng, L., Zhou, Q., Wang, Z., & Qi, M. (2022). A comprehensive review of methods based on deep learning for diabetes-related foot ulcers. Frontiers in Endocrinology, 13. https://doi.org/10.3389/fendo.2022.945020
[22] Bai, X., Li, X., Qiao, L., Wang, R., & Wu, H. (2025). Deformable kernel selection and hybrid attention fusion for airport runway foreign object debris detection. Measurement Science and Technology, 36(12), 125408. https://doi.org/10.1088/1361-6501/ae214b

[23] Jooshin, H. K., Nangir, M., & Seyedarabi, H. (2024). Inception-YOLO: Computational cost and accuracy improvement of the YOLOv5 model based on employing modified CSP, SPPF, and inception modules. Iet Image Processing, 18(8), 1985-1999. https://doi.org/10.1049/ipr2.13077
[24] Fang, C. and Yang, X. (2024). Lightweight YOLOv8 for Wheat Head Detection. Ieee Access, 12, 66214-66222. https://doi.org/10.1109/access.2024.3397556
[25] Gao, Y., Li, Z., Zhang, K., & Kong, L. (2024). GCP-YOLOv7: Lightweight underwater target detection model based on YOLOv7.. https://doi.org/10.21203/rs.3.rs-4612030/v1
[26] Shang, S., Cao, J., Wang, Y., Wang, M., Zhao, Q., Song, Y., … & Gao, H. (2024). A Dynamic Interference Detection Method of Underwater Scenes Based on Deep Learning and Attention Mechanism. Biomimetics, 9(11), 697. https://doi.org/10.3390/biomimetics9110697
[27] Ardelean, A., Ardelean, E., & Marginean, A. (2025). Can YOLO Detect Retinal Pathologies? A Step Towards Automated OCT Analysis. Diagnostics, 15(14), 1823. https://doi.org/10.3390/diagnostics15141823
[28] Ramachandran, S., George, J., Skaria, S., & V.V., V. (2018). Using yolo based deep learning network for real time detection and localization of lung nodules from low dose ct scans. Medical Imaging 2018: Computer-Aided Diagnosis, 53. https://doi.org/10.1117/12.2293699
[29] Rajasekhar, M. (2024). Understanding yolo: real-time object detection explained. Interantional Journal of Scientific Research in Engineering and Management, 08(07), 1-9. https://doi.org/10.55041/ijsrem36359
[30] Bista, R., Timilsina, A., Manandhar, A., Paudel, A., Bajracharya, A., Wagle, S., … & Ferreira, J. C. (2023). Advancing tuberculosis detection in chest x-rays: a yolov7-based approach. Information, 14(12), 655. https://doi.org/10.3390/info14120655
[31] Goswami, A. G., Verma, S., & Jangdey, M. S. (2020). Tuberculosis and its diagnosis: past, present and future. Pharmaceutical and Biosciences Journal, 33-40. https://doi.org/10.20510/ukjpb/8/i5/1606399315
[32] Fati, S. M., Senan, E. M., & ElHakim, N. (2022). Deep and hybrid learning technique for early detection of tuberculosis based on x-ray images using feature fusion. Applied Sciences, 12(14), 7092. https://doi.org/10.3390/app12147092
[33] Lakshmi, J. V. N., & Sheshasaayee, A. (2015). Machine learning approaches on map reduce for Big Data analytics. 2015 International Conference on Green Computing and Internet of Things (ICGCIoT), 480–484. https://doi.org/10.1109/ICGCIoT.2015.7380512
[34] Kishor, R. (2024). Performance benchmarking of yolov11 variants for real-time delivery vehicle detection: a study on accuracy, speed, and computational trade-offs. Asian Journal of Research in Computer Science, 17(12), 108-122. https://doi.org/10.9734/ajrcos/2024/v17i12532
[35] Sazak, H. and Kotan, M. (2024). Automated blood cell detection and classification in microscopic images using yolov11 and optimized weights. Diagnostics, 15(1), 22. https://doi.org/10.3390/diagnostics15010022
[36] Okada, K., Yamada, N., Takayanagi, K., Hiasa, Y., Kitamura, Y., Hoshino, Y., … & Kato, S. (2024). Applicability of artificial intelligence-based computer-aided detection (ai–cad) for pulmonary tuberculosis to community-based active case finding. Tropical Medicine and Health, 52(1). https://doi.org/10.1186/s41182-023-00560-6
[37] Manoli, S. N., Shariff, S., Kaliyur, K. M., Chakra, C. R., & Divith, S. (2025). Advancements in deep learning for tuberculosis detection: a review of modified cnn architectures and transfer learning approaches for chest x-ray analysis. Interantional Journal of Scientific Research in Engineering and Management, 09(03), 1-9. https://doi.org/10.55041/ijsrem42781
[38] Mahoto, N. A., Iftikhar, R., Shaikh, A., Asiri, Y., Alghamdi, A., & Rajab, K. (2021). An intelligent business model for product price prediction using machine learning approach. Intelligent Automation &Amp; Soft Computing, 29(3), 147-159. https://doi.org/10.32604/iasc.2021.018944
[39] García, R. T. M., Céspedes-López, M. F., & Perez-Sanchez, V. R. (2022). Housing price prediction using machine learning algorithms in covid-19 times. Land, 11(11), 2100. https://doi.org/10.3390/land11112100
[40] Kuo, P. and Huang, C. (2018). A high precision artificial neural networks model for short-term energy load forecasting. Energies, 11(1), 213. https://doi.org/10.3390/en11010213